

J. A. Halpin · C. L. Gerakiteys · G. L. Clarke  
E. A. Belousova · W. L. Griffin

## In-situ U–Pb geochronology and Hf isotope analyses of the Rayner Complex, east Antarctica

Received: 17 May 2004 / Accepted: 6 October 2004 / Published online: 27 November 2004  
© Springer-Verlag 2004

**Abstract** In-situ zircon U–Pb and Hf isotopic analysis via laser ablation microprobe-inductively coupled plasma mass spectrometer (LAM-ICPMS) of samples from Kemp and MacRobertson Lands, east Antarctica suggests that the Kemp Land terrane evolved separately from the rest of the Rayner Complex prior to the ca. 940 Ma Rayner Structural Episode. Several Archaean metamorphic events in rocks from western Kemp Land can be correlated with events previously reported for the adjacent Napier Complex. Recently reported ca. 1,600 Ma isotopic disturbance in rocks from the Oygarden Group may be correlated with a charnockitic intrusion in the Stillwell Hills before ca. 1,550 Ma. Despite being separated by some 200 km,  $T_{DM}^{Hf}$  ages indicate felsic orthogneiss from Rippon Point, the Oygarden Group, Havstein Island and the Stillwell Hills share a ca. 3,660–3,560 Ma source that is indistinguishable from that previously reported for parts of the Napier Complex. More recent additions to this crust include Proterozoic charnockite in the Stillwell Hills and the vicinity of Mawson Station. These plutons have distinct  $^{176}\text{Hf}/^{177}\text{Hf}$  ratios and formed via the melting of crust generated at ca. 2,150–2,550 Ma and ca. 1,790–1,870 Ma respectively.

Editorial Responsibility: T. L. Grove

J. A. Halpin (✉) · C. L. Gerakiteys · G. L. Clarke  
School of Geosciences, University of Sydney,  
Sydney, NSW, 2006 Australia  
E-mail: jacqui@geosci.usyd.edu.au  
Tel.: +61-2-93512056  
Fax: +61-2-93510184

E. A. Belousova · W. L. Griffin  
GEMOC ARC National Key Centre,  
Department of Earth and Planetary Sciences,  
Macquarie University, NSW, 2109 Australia

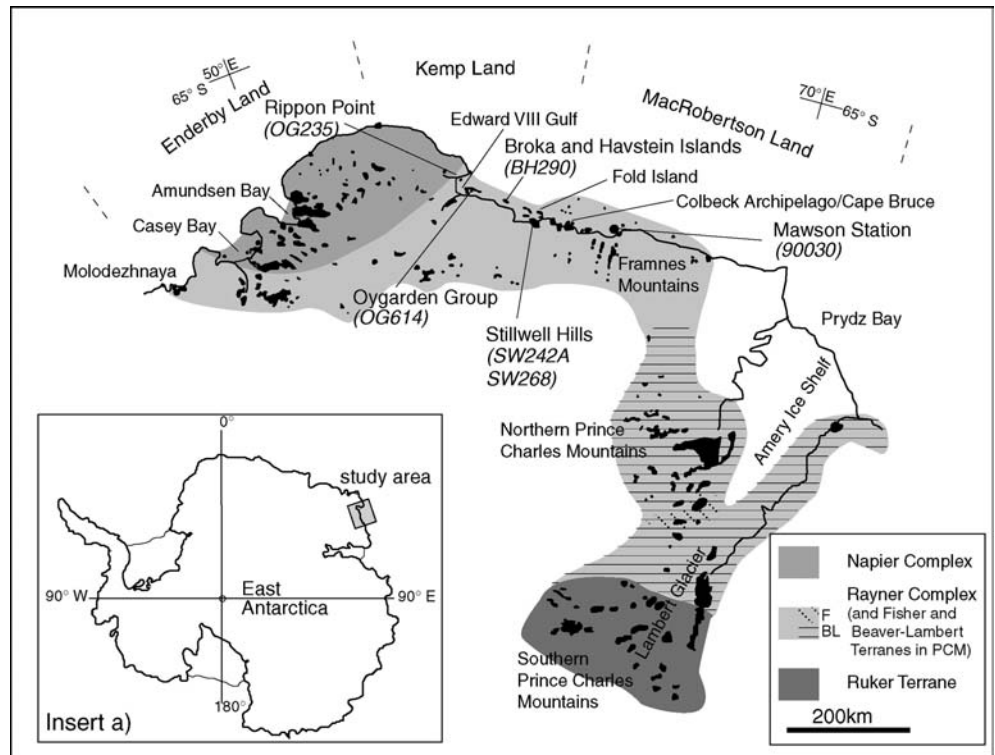
W. L. Griffin  
CSIRO Exploration and Mining,  
North Ryde, NSW, 2113 Australia

### Introduction

The coastline of MacRobertson and Kemp Lands, east Antarctica, exposes a semi-continuous profile of mid- to lower-crustal rocks of the ca. 1,000 Ma Rayner Complex (e.g. Kamenev 1972; Sheraton et al. 1987). Prior to Gondwana dispersal, rocks now exposed in this Mesoproterozoic mobile belt were contiguous with the Eastern Ghats Belt of India, both being part of a larger orogenic system that developed during the assembly of Rodinia (Fitzsimons 2000; Rickers et al. 2001). The Rayner Complex was initially defined by Kamenev (1972) to include coastal outcrops and minor inland nunataks in western Enderby Land and Kemp Land adjacent to the Archaean Napier Complex and further east into MacRobertson Land. Reconnaissance isotopic dating (Arriens 1975; Tingey 1982) recognised that this complex extends as far as the northern Prince Charles Mountains (Fig. 1).

Recent advances in laser ablation microprobe-inductively coupled plasma mass spectrometer (LAM-ICPMS) offers the possibility of combining precise U–Pb ages with in-situ analysis of Hf isotope ratios for individual zircon grains and parts of zircon grains (e.g. Griffin et al. 2000; Belousova et al. 2001; Knudsen et al. 2001). This technique can return ages with precision comparable to SHRIMP analyses (Jackson et al. 1997, 2004); when coupled with high-precision Hf-isotope analysis, this becomes a powerful tool to characterise complex terrane histories. Whereas previous geochronology studies along the Kemp and MacRobertson Land coastlines have mostly focussed on detailed work from comparatively restricted areas, this study presents the results of U–Pb and Hf analyses of zircon grains in samples from a 300 km stretch of coast in Kemp and MacRobertson Lands. Subsequent LAM-ICPMS analyses of integrated U–Pb and Hf isotopic systems are utilised in this study to investigate the spatial and temporal framework of these multiply deformed terranes.

**Fig. 1** The major geological elements of Enderby, Kemp and MacRobertson Lands. Rocks within the Rayner Complex were affected by the ca. 1,000 Ma Rayner Structural Episode. The Mesoproterozoic to early Neoproterozoic rocks of the Fisher and Beaver-Lambert Terranes of the Prince Charles Mountains are of similar age to those in the Rayner Complex. The Archaean Napier Complex and Archaean to Palaeoproterozoic Rucker Terrane are also shown. Sample locations are marked. *Insert a* Map of Antarctica showing position of study area



## Regional geology

The Napier and Rayner Complexes were initially distinguished by Kamenev (1972) on the basis of metamorphic grade: anhydrous granulite facies gneisses of the Napier Complex are bounded by lower metamorphic grade, hornblende-bearing gneisses of the Mesoproterozoic Rayner Complex (Fig. 1). Further distinctions between the two complexes involve deformed and metamorphosed mafic dykes in the Rayner Complex, thought to be equivalents of undeformed ca. 1,200 Ma dykes in the Napier Complex (e.g. Sheraton et al. 1980; Sheraton and Black 1981; Clarke 1988). This division is now mostly based on extensive isotopic data (e.g. Sheraton and Black 1983; Black et al. 1987; Sheraton et al. 1987; Harley and Black 1997; Dunkley 1998; Kelly 2000; Carson et al. 2002; Dunkley et al. 2002; Kelly et al. 2002; Hokada et al. 2003). The Napier Complex includes felsic igneous precursors to orthogneisses as old as ca. 3,800 Ma (Black et al. 1986; Harley and Black 1997), but most lithologies were formed or metamorphosed during the late Archaean (e.g. Sheraton et al. 1987; Harley and Black 1997; Hokada et al. 2003). At least three major deformation episodes have been identified (e.g. Sandiford and Wilson 1984; Sheraton et al. 1987; Harley and Black 1997), but the timing of peak UHT metamorphism is controversial. Zircon ages from syn-metamorphic pegmatites led Grew and Manton (1979) to infer that ca. 2,500 Ma high-grade metamorphism affected a large portion of the Napier Complex. An emplacement age for a syn- $D_1$  orthogneiss lead Harley and Black (1997) to infer that UHT metamorphism occurred at ca.

2,840 Ma ( $D_1$ ,  $D_2$ ) and lower-temperature transitional granulite facies metamorphism occurred at ca. 2,450 Ma ( $D_3$ ). In contrast, other workers interpret the younger ca. 2,480–2,450 Ma age to represent the UHT event (e.g. Grew 1998; Carson et al. 2002; Hokada et al. 2003, 2004). Zircon data from locally discordant leucosome was used to constrain UHT metamorphism to be older than 2,590–2,550 Ma by Harley et al. (2001). These workers suggest that the numerous ca. 2,500–2,450 Ma ages represent post-UHT events. Hokada et al. (2004) concede that though their geochronological data support UHT metamorphism ca. 2,480–2,475 Ma, they do not exclude the possibility of another ca. 2,590–2,550 Ma high-grade (possibly UHT) event as inferred by Harley et al. (2001)

The eastern boundary of the Napier Complex mostly involves a Neoproterozoic strain gradient, with much of the Rayner Complex in Kemp Land interpreted to represent Archaean crust tectonically reworked during the Rayner Structural Episode (RSE) between 1,000 and 900 Ma (Table 1). Rb-Sr whole rock isochrons give an age of ca. 3,070 Ma for a depleted tonalite and ca. 2,500 Ma for a depleted granite and garnet gneiss from Edward VIII Gulf (Fig. 1; Sheraton and Black 1983). These are interpreted to reflect Archaean protoliths that underwent isotopic disturbance at ca. 2,500 Ma (Grew and Manton 1979; Sheraton and Black 1983; Sheraton et al. 1987). U-Pb SHRIMP data from zircons in two generations of felsic orthogneisses in the Oygarden Islands (Fig. 1) give minimum crystallisation ages of ca. 3,650 and 2,780 Ma respectively, both rocks having potentially suffered ca. 24,00 Ma isotopic disturbance



Table 1 (Contd.)

Age (Ma)	Western Enderby Land	Age (Ma)	Kemp Land	Age (Ma)	Mawson Coast	Age (Ma)	Northern Prince Charles Mountains
1,488 + 19/-16	Anorthosite —Amphitheatre Lake (U-Pb) <sup>g</sup>					1,604	Charnockite—Mt McCarthy (T <sup>Nd</sup> <sub>DM</sub> ) <sup>e</sup>
1,465 + 25/-20	Granitic orthogneiss —Mt Flett (U-Pb) <sup>g</sup>					1,597	Metapelite—White Massif (T <sup>Nd</sup> <sub>DM</sub> ) <sup>e</sup>
1,425 + 29/-27	Granitic orthogneiss —Thala Hills (U-Pb) <sup>g</sup>					1466–1735	Granite ± monzonite —Mt Collins (T <sup>Nd</sup> <sub>DM</sub> ) <sup>e</sup>
1,290	Granite orthogneiss —Mt Underwood (T <sup>Nd</sup> <sub>DM</sub> ) <sup>g</sup>	ca. 1,300–2,000		ca. 1,300–2,000	Orthogneiss—Cape Bruce (U-Pb) <sup>q</sup>	1,293 ± 28	Granodiorite—Fisher Massif (U-Pb) <sup>d</sup>
		1,256 ± 17	Felsic paragneiss—Stillwell Hills (Rb-Sr w. r. isochron) <sup>e</sup>	1,254 ± 31	Banded gneiss —Framnes Mountains (Rb-Sr w. r. isochron) <sup>j</sup>	1,283 ± 21	Metadacite—Fisher Massif (U-Pb) <sup>d</sup>
				1,153 ± 47	Banded gneiss—Framnes Mountains (Rb-Sr w. r. isochron) <sup>j</sup>		
1,022 ± 60	Granitic orthogneiss —Thala Hills (Rb-Sr w. r. isochron) <sup>k</sup>					1,020 ± 48	Biotite granite—Fisher Massif (U-Pb) <sup>d</sup>
						1,017 ± 31	Leucosome—Radok Lake (U-Pb) <sup>l</sup>
						1013 ± 31	pegmatite—Mt Kirkby (U-Pb) <sup>m</sup>
						1000 + 14/-11	orthogneiss—Jetty Peninsula (U-Pb) <sup>n</sup>
						998 ± 38	charnockite—White Massif (Rb-Sr w. r. isochron) <sup>e</sup>
		992 ± 10			biotite-orthopyroxene orthogneiss—Cape Bruce (U-Pb) <sup>o</sup>	991 ± 22	pegmatite—Mt Kirkby (U-Pb) <sup>m</sup>
						990 ± 30, 994 ± 39	leucogneiss—Mt McCarthy (U-Pb) <sup>d</sup>
						990 ± 18	granite—Radok Lake (U-Pb) <sup>l</sup>
						984 ± 12	syenite—Mt Collins (U-Pb) <sup>d</sup>
						984 ± 7	granite—Mt Collins (U-Pb) <sup>d</sup>
		954 ± 12, 985 ± 29			charnockite—Mawson Station (U-Pb) <sup>n</sup>	980 ± 21	monzonite—Loewe Massif (U-Pb) <sup>d</sup>
						976 ± 25	granite—Mt Collins (U-Pb) <sup>d</sup>
						942 ± 17	leucosome—Baitye Glacier (U-Pb) <sup>l</sup>
		937 ± 19	pegmatite—Fold Island (U-Pb) <sup>p</sup>		felsic dyke—Cape Bruce (U-Pb) <sup>o</sup>	940 + 24/-17	gneissic leucogranite —Jetty Peninsula (U-Pb) <sup>n</sup>

923 + 6/-7	Granitic orthogneiss-Mt Flett (U-Pb) <sup>7</sup>	931 ± 14	pegmatite—Oygarden Islands (U-Pb) <sup>j</sup>	935 + 3700/-12	charnockite—Mawson Station (U-Pb) <sup>g</sup>	936 ± 14	granite—Radok Lake (U-Pb) <sup>j</sup>
		929 ± 12, 924 ± 17	felsic orthogneiss—Oygarden Islands (U-Pb) <sup>j</sup>				
		913 ± 8	charnockite—Stillwell Hills (U-Pb) <sup>i</sup>	921 ± 19	charnockite—Mawson Station (U-Pb) <sup>h</sup>		
		904 ± 16	felsic migmatite—Oygarden Islands (U-Pb) <sup>j</sup>	ca. 910	paragneiss, orthogneiss, pegmatite—Cape Bruce (U-Pb) <sup>o</sup>	910 ± 18	pegmatite—Mt Kirkby (U-Pb) <sup>m</sup>
		884 ± 24	felsic migmatite—Oygarden Islands (U-Pb) <sup>i</sup>	886 ± 48	charnockite—Mawson Station (Rb-Sr w. r. isochron) <sup>g</sup>	900 ± 28	leucosome—Radok Lake (U-Pb) <sup>j</sup>
892 + 90/-14	Paragneiss-Mt Underwood (U-Pb, monazite) <sup>7</sup>	844 ± 24	pegmatite—Oygarden Islands (U-Pb) <sup>j</sup>				

References: (a) Kelly 2000; (b) Sheraton and Black 1983; (c) Clarke 1987; (d) Kinny et al. 1997; (e) Zhao et al. 1997; (f) Young et al. 1997; (g) Black et al. 1987; (h) Young and Black 1991; (i) Kelly et al. 2002; (j) Arriens, unpub., recal. in Young and Black 1991; (k) Grew 1978 recal. in Sheraton et al. 1987; (l) Boger et al. 2000; (m) Carson et al. 2000; (n) Manton et al. 1992; (o) Dunkley et al. 2002; (p) Grew et al. 1988; (q) Dunkley 1998; (r) Grew and Manton 1979. Ages younger than ca. 800 Ma have not been included. *Grey shaded areas* refer to extent of the RSE as inferred from previous geochronology

(Kelly 2000). A poorly constrained U–Pb age of  $3,081 \pm 170$  Ma for a quartzofeldspathic gneiss from Fold Island (Fig. 1) was interpreted by Grew et al. (1988) to reflect xenocrystic zircon. In the Stillwell Hills (Fig. 1), a Rb–Sr isochron age of  $2,692 \pm 48$  Ma for a felsic orthogneiss may represent a crystallisation age of the igneous protolith and/or a metamorphic event (Clarke 1987).

In contrast to these Archaean ages from orthogneiss in Kemp Land, rocks in western Enderby Land, along the Mawson Coast and in the northern Prince Charles mountains (nPCM; Fig. 1) mostly give Mesoproterozoic ages (Table 1). Gneiss and granite in western Enderby Land yield  $T_{DM}^{Nd}$  ages between 2,180 and 1,290 Ma (Black et al. 1987). U–Pb ages of xenocrystic zircon grains in orthogneiss further east at Cape Bruce (MacRobertson Land, Fig. 1) mostly lie between 2,000 and 1,300 Ma (Dunkley 1998).  $T_{DM}^{Nd}$  ages between 2,170 and 1,600 Ma are reported for charnockite bodies along the Mawson Coast as well as the nPCM (Young et al. 1997; Zhao et al. 1997). Gneisses in the nPCM have inherited zircon grains that give ca. 1,900 and 1,850 Ma U–Pb ages (Kinny et al. 1997). A paragneiss at Mt Meredith (nPCM) records an inherited/detrital zircon population of Archaean age (2,800–2,500 Ma), which is possibly sourced from the southern PCM (Kinny et al. 1997). U–Pb zircon ages for felsic gneiss xenoliths, pillars and roof pendants within a large charnockitic body at Mawson Station mostly lie between ca. 2,000–1,700 Ma (Young and Black 1991).

The onset of the RSE in the Rayner Complex (Table 1) was marked by granulite facies metamorphism and deformation, and extensive felsic magmatism along the Mawson Coast and in the nPCM (e.g. Young and Black 1991; Kinny et al. 1997; Young et al. 1997; Dunkley 1998; Boger et al. 2000; Carson et al. 2000; Dunkley et al. 2002). The RSE is first recorded between ca. 1,000–980 Ma in MacRobertson Land. Relative ages for successive felsic plutons at Cape Bruce (Fig. 1) can be qualitatively constrained by field criteria (Dunkley 1998). These give poorly resolved U–Pb SHRIMP ages from zircons, consistent with early magmatism and peak granulite facies metamorphism (local  $M_1$ – $D_1$ ) at ca. 990 Ma and later magmatism and subtly lower temperature metamorphism (local  $M_2$ – $D_2$ ) between ca. 990 and 960 Ma (Dunkley 1998). The emplacement of large charnockite bodies along the Mawson Coast immediately followed peak metamorphic conditions at  $985 \pm 29$  and  $954 \pm 19$  Ma (Young and Black 1991). U–Pb zircon ages for both mantle-derived and intracrustal plutons from the nPCM reflect a major ca. 990–980 Ma magmatic event, which accompanied the onset of peak granulite facies conditions in that area (Kinny et al. 1997; Boger et al. 2000; Carson et al. 2000). Post-charnockite deformation occurred in the nPCM at ca. 940 Ma (Manton et al. 1992; Boger et al. 2000). The last phase of the RSE affected this area at ca. 910–900 Ma (Boger et al. 2000; Carson et al. 2000). At Mawson Station, ca. 920 Ma zircon rims from the charnockite are



interpreted to represent the effects of metamorphism that post-dated charnockite emplacement (Young and Black 1991).

Kemp Land does not appear to have been affected by the RSE until ca. 940–900 Ma, a time that correlates with the waning stages of deformation in MacRobertson Land. A poorly constrained U–Pb age of  $940 \pm 80$  Ma for a syn-tectonic pegmatite at Fold Island north of the Stillwell Hills records the earliest evidence for the RSE in this area (Grew et al. 1988). A U–Pb SHRIMP age of  $913 \pm 8$  Ma for zircon from the Stillwell Hills charnockite is interpreted as a metamorphic age (Kelly et al. 2002). In the Oygarden Islands (Fig. 1), metamorphic overgrowths on zircon from a felsic orthogneiss and a syn-deformational pegmatite yield ca. 930 Ma U–Pb ages (Kelly et al. 2002). Whereas Kemp Land shows evidence for metamorphic activity during the late RSE, it lacks evidence for deformation and metamorphic events in the period ca. 1,000–940 Ma. Kelly et al. (2002) suggest this may be indicative of a two-stage structural evolution for the Rayner Complex during the RSE.

## Analytical procedure

### Sample preparation and imaging

Samples were crushed and zircon grains separated using magnetic separation and heavy liquids at the CSIRO laboratories in North Ryde. Zircon grains were then hand picked and mounted in epoxy discs and polished so as to just reveal the central portions of the grains at the GEMOC Key Centre, Macquarie University. Each zircon grain was imaged using cathodoluminescence imagery at the University of Technology, Sydney. Prior to analysis by LAM-ICPMS, each zircon grain was analysed by electron microprobe at the Electron Microprobe Unit, University of New South Wales. Two runs were carried out on each grain: a major suite of elements including Zr, Hf, and Si, and a trace suite of elements including Y, Hf, Th, and U. Mounts and standards were cleaned in 2 M nitric acid for approximately 1 h before laser analysis. Many zircons were large enough to allow the Pb and Hf analyses to be carried out on the same grain. However care was taken to ensure the beam did not sample a combination of both core and rim components (if applicable to a specific grain) during these analyses. Zircons too small for both Pb and Hf analyses were analysed for Pb exclusively and used only in constructing the U–Pb concordia plots.

### U–Pb isotope analysis

U–Pb analysis was performed using a custom-built 266 nm UV LAM (Norman et al. 1996), coupled to an Agilent HP4500 series 300 ICPMS at the GEMOC Key Centre, Macquarie University. Analytical methods employed in this study follow closely those described by

Spetsius et al. (2002). For a detailed discussion of the procedures involved in in-situ U–Pb zircon geochronology using LA-ICP-MS see Jackson et al. (2004).

Accurate ages are dependent on the minimization of elemental fractionation effects as well as inherent mass bias of the mass spectrometer itself. Ablation of standards and samples in He was employed to increase sample transport efficiency, decrease ablation product deposition and to stabilise signals. Focussing of the laser above the sample allowed for the effects of dynamic U/Pb fractionation during laser beam penetration (Hirata and Nesbitt 1995) to be reduced. Operating conditions (Table 2) for the laser were kept stable to ensure constant U/Pb fractionation. Calibration against a standard zircon GJ-1 (Jackson et al. 2004) involved a typical ‘run’ of four analyses of this standard, followed by analyses of two near-concordant zircons 95100 (Wiedenbeck et al. 1995) and Mud Tank (Black and Gulson 1978) as an independent control. Analysis of up to ten unknowns followed initial calibration, followed by four further analyses of the GJ-1 standard which allows for suitable correction for drift.

Background measurements were taken for ca. 60 s prior to ablation of the sample. Peak hopping at short dwell times on five isotopes ( $^{206}\text{Pb}$ ,  $^{207}\text{Pb}$ ,  $^{208}\text{Pb}$ ,  $^{232}\text{Th}$  and  $^{238}\text{U}$ ) allowed for measurement of the five masses almost simultaneously. Data acquisition involved the analysis of time-resolved signals (which corresponds to ablation-depth profiles) and allowed identification of isotopic heterogeneity within the ablation volume. Output signals for each analysis are automatically matched to signals from the standard zircons during the same time interval, allowing for optimal signal interval selection. Acquisition parameters are shown in Table 2. Ablation pits are 40–50  $\mu\text{m}$  in diameter (shown in Fig. 2a).

Raw data were manipulated using the in-house GLITTER data reduction program which calculates isotopic ratios ( $^{207}\text{Pb}/^{206}\text{Pb}$ ,  $^{208}\text{Pb}/^{232}\text{Th}$ ,  $^{208}\text{Pb}/^{238}\text{U}$  and  $^{207}\text{Pb}/^{235}\text{U}$  where  $^{235}\text{U} = ^{238}\text{U}/137.88$ ) for the selected portion of each ablation. Net background-corrected count rates for each isotope were used for age calculations. The program ComPbCorr of Anderson (2002) was employed to correct for small contributions of common Pb in the zircons analysed. Concordia diagrams and age calculations were made using ISOPLOT 2.49 v (Ludwig 2001). Uncertainties for individual analyses as quoted in tables and text, and as error ellipses on standard Wetherill concordia plots have been calculated to the one-sigma level. Weighted average age calculations are reported at 95% confidence limits.

### Hf isotope analysis

Hafnium isotope analysis was carried out in-situ using a Merchantek EO LUV213 LAM attached to a Nu Plasma multi-collector ICPMS at GEMOC. Methodology follows that described in detail by Griffin et al. (2000)

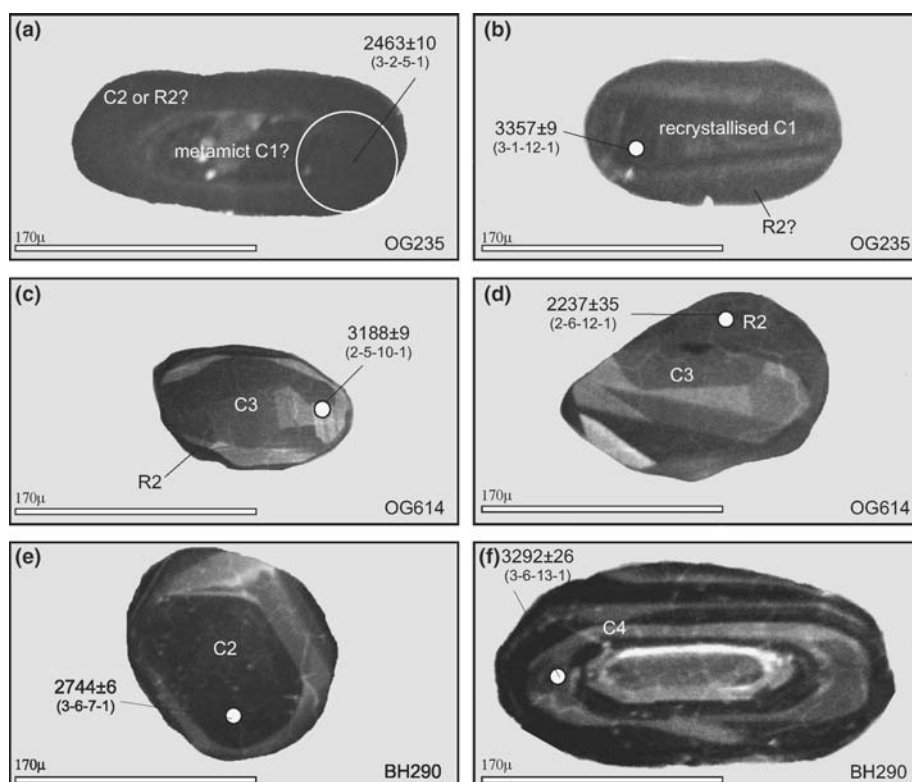
**Table 2** LAM-ICPMS operating conditions and data acquisition parameters

ICPMS		
Model	Agilent 4500	
Forward power	1,350 kW	70% power output
Gas flows		
Plasma	Ar 16 l/min	
Auxiliary	Ar 1 l/min	
Carrier	He 0.9–1.2 l/min, Ar 0.9–1.2 l/min	
Expansion chamber pressure	350–360 Pa <sup>a</sup>	
LAM	Custom system	213 Merchanteck <sup>b</sup>
Wavelength	266 nm	213 nm
Repetition rate	10 Hz	5 Hz
Pre-ablation laser warm up	Laser fired continuously	None
Pulse duration (FWHM)	9 ns	5 ns
Aperture beam diameter/iris setting	4 nm	30%
Beam expander setting	NA	30
Focusing objective	×10, f.1 = 20 mm	×5, f.1 = 40 mm
Degree of defocusing	150–500 mm (above sample)	
Spot size	60–80 mm	40–50 mm
Incident pulse energy	ca. 0.8 mJ	ca. 0.1 mJ
Energy density on sample	ca. 12 J/cm <sup>2</sup>	ca. 8 J/cm <sup>2</sup>
Data acquisition parameters		
Data acquisition protocol	Time-resolved analysis	
Scanning mode	Peak hopping, one point per peak	
Detector mode	Pulse counting	
Isotopes detected	<sup>206</sup> Pb, <sup>207</sup> Pb, <sup>208</sup> Pb, <sup>232</sup> Th, <sup>238</sup> U	
Dwell time per isotope	15, 30, 10, 10, 15 ms respectively	
Quadruple settling time	ca. 2 ms	
Time/scan	ca. 89 ms	
Data acquisition time	ca. 180 s	
Samples and standards		
Samples	Hand-picked, high-quality zircon grains	
Mounts	25 mm-diameter polished grain mounts	
Standards	GJ-1, 91500, Mud Tank	

<sup>a</sup>Pirani vacuum gauge may not be calibrated accurately for Ar/He mixtures

<sup>b</sup>Laser system set-up for Hf analyses

**Fig. 2** Cathodoluminescence (CL) images of zircons from orthogneiss samples OG235, OG614 and BH290. The average ablation pit size (~70 μm) for the 266 nm laser is shown in Fig. 2a. **a** Homogeneous C2 core (or R2?) with low CL which encloses a corroded and possibly metamict C1 core (OG235). **b** 'Blurred' oscillatory zoning which is typical of partially recrystallised C1 cores. The core is surrounded by an ?R2 rim (OG235). **c** Rounded C3 core showing sector zoning and some planar growth banding, surrounded by a homogeneous, low-CL R2 rim (OG614). **d** Sector zoned C3 core surrounded by a thick, homogeneous R2 rim (OG614). **e** Largely homogeneous low CL and rounded C2 core (BH290). **f** Broad concentric zoning of a C4 core (BH290)



and laser operating conditions are listed in Table 2. Ablation pits for the 213 nm laser beam are 60–80  $\mu\text{m}$ . Interference of  $^{176}\text{Lu}$  on  $^{176}\text{Hf}$  has been corrected by measuring the intensity of the interference-free  $^{175}\text{Lu}$  using  $^{176}\text{Lu}/^{175}\text{Lu}=0.02669$  (De Bièvre and Taylor 1993) to calculate  $^{176}\text{Lu}/^{177}\text{Hf}$ . Interference of  $^{176}\text{Yb}$  on  $^{176}\text{Hf}$  was corrected by measuring the interference-free  $^{172}\text{Yb}$  isotope and using  $^{176}\text{Yb}/^{172}\text{Yb}$  to calculate  $^{176}\text{Yb}/^{177}\text{Hf}$ . The precision and accuracy of these analyses is highlighted by analysis of zircon standards discussed in detail in Griffin et al. (2000).

Like the U–Pb analyses discussed previously, laser-ablation Hf analyses were carried out using time-resolved analysis software which allows uniform portions of the output signals to be selected. The calculation of  $\epsilon\text{Hf}$  values used the  $^{176}\text{Lu}$  decay constant of Blichert-Toft et al. (1997). This value of  $1.93\times 10^{-11}$  lies between the two other published values (Scherer et al. (2001) and Bizzarro et al. (2003);  $1.865\times 10^{-11}$  and  $1.983\times 10^{-11}$  respectively). Calculated model ages are based on the depleted mantle model described by Griffin et al. (2000).

### Sample descriptions

Locations of the six samples used in this study are shown on Fig. 1. Sample OG235 from Rippon Point in the Napier Complex, west of the Oygarden Group, is from a homogenous felsic orthogneiss that cuts a local  $S_1$  foliation and preserves an intense  $S_2$  foliation defined by orthopyroxene, quartz and feldspar. Sample OG614 was taken from a felsic layer within a layered composite orthogneiss (Kelly et al. 2000, 2002) from the Oygarden Group (Fig. 1). It contains a coarse-grained  $S_1$  gneissic foliation defined by elongate quartz and feldspar grains, with trails of garnet and orthopyroxene. It is the oldest lithology of the Oygarden Group; U–Pb SHRIMP ages for zircon grains from a sample from the same outcrop (OG615) are presented by Kelly (2000). Sample BH290 was taken from a homogeneous felsic orthogneiss of which the majority of both Broka and Havstein Islands (Fig. 1) are formed. Trails of garnet and/or orthopyroxene, quartz and feldspar define a locally pervasive  $S_2$  foliation that is cut by pre- $D_3$  mafic dykes.  $S_2$  and the mafic dykes are commonly transposed into  $S_3$ . Two samples were taken from the Stillwell Hills (Fig. 1). SW268 is a sample of the Stillwell Hills Orthogneiss, which is the main lithology in the southern Stillwell Hills (Stillwell Gneiss of Clarke 1988). A dominant  $S_2$  foliation is defined by alternating felsic and mafic layers: quartz-K-feldspar-plagioclase-pyroxene-bearing orthogneiss is finely interbanded with pyroxene-hornblende-plagioclase  $\pm$  garnet mafic gneiss. Sample SW242A was taken from a K-feldspar-megacrystic charnockite in the Stillwell Hills (the same lithology as SW242 of Kelly et al. 2002). This charnockite cuts  $S_2$  in the Stillwell Hills, and is itself cut by the pre- $D_3$  mafic dykes. Igneous textures are preserved in areas of low  $D_3$  strain. The sample used in this study was taken from an area of low

$D_3$  strain and contains large K-feldspar megacrysts to up to 6 cm in length. Sample 90030 was taken from a K-feldspar megacrystic charnockite at Mawson Station (Mawson Charnockite of Trail 1970). The charnockite cuts a granulite facies  $S_2$  foliation in metasedimentary xenoliths and pillars of the Painted Gneiss (Clarke 1988), and is typically massive. It preserves evidence of two foliations,  $S_3$  and  $S_4$ . Sample 90030 is massive and contains K-feldspar megacrysts to 3 cm in length.

### Results

#### Texturally defined zircon types and Th/U chemistry

Under transmitted light, the zircon grains are colourless to pale honey or brown, with localised domains rich in inclusions common in grain cores. Scanning electron microscope (SEM) imaging delineated internal zonation patterns, which are commonly complex and reflect repeated stages of growth and/or recrystallisation during metamorphic events. Given the similarity of zircons, and the overlap of some sample locations, the classification of the zircons analysed in this study follows that established by Kelly (2000) with minor variations as listed in Table 3. Optical analysis revealed four core and two rim types (Table 3) with some minor variation between samples.

In OG235, zircons vary in width from  $\sim 170$  to  $\sim 300$   $\mu\text{m}$ , and are typically elongate to sub-rounded, with consistently rounded terminations. Some possible C2 cores (or R2 rims?) are unusual in that they contain commonly eroded, possibly C1 metamict cores (Fig. 2a). Some C1 cores exhibit ‘blurred’ oscillatory zoning (Fig. 2b) and are interpreted to be recrystallised igneous zircon grains or grain relicts (Pidgeon et al. 1998; Hoskin and Black 2000).

Zircon grains in sample OG614 are consistently rounded, with some sub-rounded zircon fragments of C3 cores and range in size from  $\sim 80$  to  $\sim 250$   $\mu\text{m}$ . R2 rims are commonly developed though many are too fine to be analysed separately ( $\sim 8$   $\mu\text{m}$  wide). C3 sector zoning, and lesser planar growth banding, is very well developed in all samples (Fig. 2c, d). This type of mixed zoning is interpreted to result from fluctuating crystal growth rates and is commonly observed in zircons that have crystallised from or grown in the presence of melt during high-grade metamorphism (Vavra et al. 1996; Rubatto et al. 1998; Schaltegger et al. 1999; Vavra et al. 1999; Kelly et al. 2002).

Zircon in sample BH290 is  $\sim 130$  to  $\sim 260$   $\mu\text{m}$  in size. All types are predominantly elongate with rounded terminations, with some rounded to sub-rounded C2 (Fig. 2e) and C3 cores. The C1 and C4 cores are elongate, with the C1 cores showing oscillatory zoning and the C4 cores preserving broad concentric zonation (Fig. 2f). These C4 cores are interpreted to have formed or modified during metamorphism.

In sample SW268, zircons mostly have C1 and black C1 cores. Typically, they are elongate with sub-rounded



**Table 3** Zircon core and rim classification as interpreted by CL imaging and morphology

Zircon type	Description	CL response	Interpretation	Samples
C1	Common oscillatory zoning, may get 'ghost' structures, mostly elongate, some stubby with rounded terminations, black cores common in sample SW268	Moderate to low	Magmatic, may be partially recrystallised or modified	OG235, SW268, BH290, SW242A, 90030
C2	Homogenous, may get faint/patchy zoning, commonly rounded/stubby	Low to moderate	Metamorphic and highly modified magmatic grains	OG235, BH290
C3	Most diverse internal zoning; radial and irregular sector zoning, planar growth banding	Low to moderate	Crystallised from/grown in presence of anatectic melt at high temperatures	OG235, OG614, BH290, SW238, SW242A, 90030
C4	Broad concentric zoning, stubby to elongate	Moderate to low	Metamorphic recrystallisation/growth	OG235, BH290
R1	'Bleached' appearance, broadly homogeneous, may preserve patchy concentric zoning	Moderate to high	Recrystallisation/modification of pre-existing zircon during metamorphism	SW242A, 90030
R2	Variable thickness and often discontinuous, homogeneous	Moderate to low	Growth of new zircon during metamorphism	OG614, BH290

terminations and vary in size from  $\sim 140$  to  $\sim 300$   $\mu\text{m}$ . A few samples preserve fine, bright R1 rims. Almost all of the grains contain a large black, homogenous core (Fig. 3a). Such C1 cores are interpreted to be metamict as they usually yield a younger age than that obtained from the surrounding oscillatory-zoned material. One zircon, which has a moderately high CL response with faint (remnant?) sector zonation and planar growth banding or recrystallisation fronts towards the rim, is interpreted as a C3 core (Fig. 3b).

C1 cores dominate zircon in sample SW242A, and range in size from  $\sim 150$  to  $\sim 315$   $\mu\text{m}$ . The C1 core zircons are typically elongate with sub-rounded to angular edges and are often totally enclosed by a bright R1 rim (Fig. 3c). These brightly luminescent seams or 'bleached' regions have been interpreted as a result of late-stage recrystallisation by other workers (e.g. Vavra et al. 1996; Schaltegger et al. 1999). Other R1 rims are thick and display oscillatory zoning (Fig. 3d). Rims such as these have been described by workers such as Schaltegger et al. (1999) and Hoskin and Black (2000) and are interpreted to have formed through recrystallisation of the original magmatic zircon.

Zircons in sample 90030 mostly have C1 and C3 cores. C1 cores are typically elongate with sub-rounded terminations, and up to  $\sim 370$   $\mu\text{m}$  long. 'Blurred' zonation suggests recrystallisation in many of the C1 cores. C3 cores are dominated by sector zonation and planar growth banding (Fig. 3e), with one C3 core with faint zonation growing around a C1 core (Fig. 3f).

Figure 4a illustrates the Th–U ratios for all analyses grouped by samples, whereas Fig. 4b shows the Th–U ratio by zircon type. Though there is overlap of U–Th concentrations in zircon from the various lithologies, some broad trends can be seen in Fig. 4a. Zircon grains from charnockite have the highest Th/U ratios (SW242A–Th/U $\approx 0.5$ –7.2; 90030–Th/U $\approx 0.2$ –2.2), whereas zircon from the orthogneiss samples (BH290, OG235, OG614, SW268) have markedly lower Th/U ratios (Th/U $\approx 0.04$ –

0.9). C1 cores have highest Th/U $\approx 0.07$ –7.2; partially recrystallised and/or metamict C1 cores plot at the lower end of this Th/U range (Fig. 4b). R1 rims have Th/U $\approx 0.61$ –2.27. These values lie within typical 'magmatic' ratios (Th/U > 0.4; Rubatto and Gebauer 2000) and probably reflect modification of magmatic zircon (C1). C3 cores span an intermediate range from Th/U $\approx 0.09$ –2.16 and may be explained via fluctuating element budgets during partial melting. Metamorphic C2 (Th/U $\approx 0.04$ –0.47) and C4 (Th/U $\approx 0.06$ –0.23) cores and R2 (Th/U $\approx 0.07$ –0.50) rims plot at low Th/U ratios, but span a greater range than typical 'metamorphic' zircon (Th/U $\approx 0.05$ –0.1; Rubatto and Gebauer 2000). This suggests recrystallisation or annealing processes, rather than new zircon growth, are probably responsible for much of the metamorphic zircon analysed in this study.

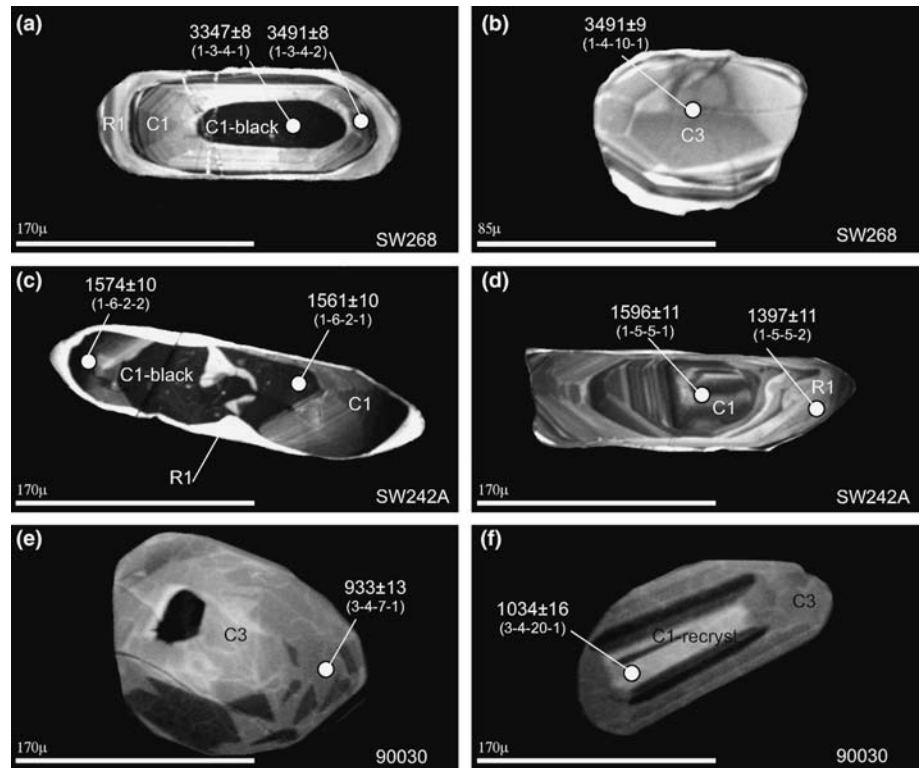
#### U–Pb age data

Zircon grains in rocks from Kemp and MacRobertson Land record complex histories with several periods of isotopic disturbance and multiple growth stages (Dunkley 1998; Kelly 2000; Kelly et al. 2002). The interpretation of discordant U–Pb ages from such rocks with poly-phase high-grade metamorphic histories is difficult. The calculation of discordia regressions often incurs large errors due to the interpolation of the data required. As discussed by Mezger and Krogstad (1997), the lower and upper intercept of such regressions may have no geological significance. For complex data reported below, chords are only calculated for samples with close to concordant data.

#### *OG235 - pre-D<sub>2</sub> homogenous felsic orthogneiss, Rippon Point*

Thirty analyses of thirty zircon grains were obtained for sample OG235 (ETable 1; Electronic Supplementary Material). Figure 5a presents the isotopic data on a

**Fig. 3** Cathodoluminescence images of zircon grains from orthogneiss samples SW268, SW242A and 90030. **a** Black C1 core surrounded by a high CL oscillatory zoned C1 core and a faintly zoned R1 rim. Ages indicate metamict black C1 core to be younger than the surrounding oscillatory zoned core (SW268). **b** Faintly zoned C3 core with moderately high CL response and oscillatory zoning at rim (SW268). **c** Partially recrystallised black C1 core surrounded by a C1 core and a high CL R1 rim that truncates oscillatory zoning and embays core (SW242A). **d** C1 oscillatory zoned core surrounded by a recrystallised (higher CL) R1 rim (SW242A). **e** Sector zoned, 'soccer-ball' type C3 core that encloses a small, possible inherited core (90030). **f** Partially oscillatory-zoned C1 core that is recrystallised and surrounded by a C3 core (90030)



Wetherill concordia diagram. The oldest concordant age (number 6; C1) is  $3,532 \pm 8$  Ma. Another oscillatory zoned C1 core has a concordant age of  $3,518 \pm 9$  Ma (number 16). Whereas these zircons have an oscillatory zoned core that is truncated and embayed by an (R1?) overgrowth, there is no clear evidence that these C1 cores are xenocrystic. Several concordant and near concordant C3 analyses and one C2 analysis cluster at ca. 3,430–3,400 Ma with the remaining zircon analyses spread out along or near concordia. An error-weighted mean (inset Fig. 5a) of seven ages from a tight cluster comprising exclusively C2 zircons gives an age of  $2,468 \pm 7$  Ma.

As indicated by previous studies (e.g. Sheraton et al. 1980, 1987), Rippon Point is part of the Archaean Napier Complex.  $^{207}\text{Pb}/^{206}\text{Pb}$  ages indicate a crystallisation age older than ca. 3,430 Ma and probably ca. 3,530 Ma. The concordant cluster of ca. 3,430–3,400 Ma C2 and C3 cores may indicate recrystallisation or new zircon growth. However there is no evidence of an event at this time elsewhere in the Napier Complex. Two concordant metamorphic zircon  $^{207}\text{Pb}/^{206}\text{Pb}$  ages of  $2,809 \pm 9$  and  $2,798 \pm 9$  Ma may represent zircon growth or modification during a metamorphic event, though this age is rather speculative as it is based on only a two concordant ages. Metamorphism in the Napier Complex has been interpreted to have occurred between ca. 2,850–2,790 Ma by Hokada et al. (2003) on the basis of  $^{207}\text{Pb}/^{206}\text{Pb}$  zircon ages from two felsic orthogneiss samples from Mt. Riiser-Larsen. Kelly and Harley (2004) have combined SEM imaging and trace/rare

earth element chemistry of zircons to reanalyse and reinterpret samples originally dated by Harley and Black (1997). Their reinterpretation has ca. 2,850–2,840 Ma metamorphic zircon growth unrelated to UHT metamorphism, in contrast to the interpretation presented by Harley and Black (1997). A cluster of ca. 2,470 Ma C2 metamorphic cores in OG235 compare well with ca. 2,500–2,450 Ma estimates for the timing of UHT metamorphism as proposed by several studies (e.g. Grew and Manton 1979; Grew 1998; Carson et al. 2002; Hokada et al. 2003, 2004). However, a concordant zircon population at this time does not preclude other estimates of UHT metamorphism (Harley et al. 2001; Kelly and Harley 2004). It is consistent with a metamorphic event at this time, the nature of which cannot be interpreted from these data.

#### *OG614 - pre-D<sub>1</sub> felsic orthogneiss, Alphard Island, Oygarden Group*

Eighteen analyses were made of 17 zircons from sample OG614 (ETable 2; Electronic Supplementary Material) and results are shown on a Wetherill concordia diagram (Fig. 5b). Discordance in this sample is complex and the data are interpreted to reflect several periods of isotopic mobilisation. The oldest concordant analysis has a  $^{207}\text{Pb}/^{206}\text{Pb}$  age of  $3,554 \pm 9$  Ma (number 3; C3) and the remaining data define a trend towards the ages of two metamorphic R2 rims (numbers 10 and 17) at ca. 1,200 Ma.

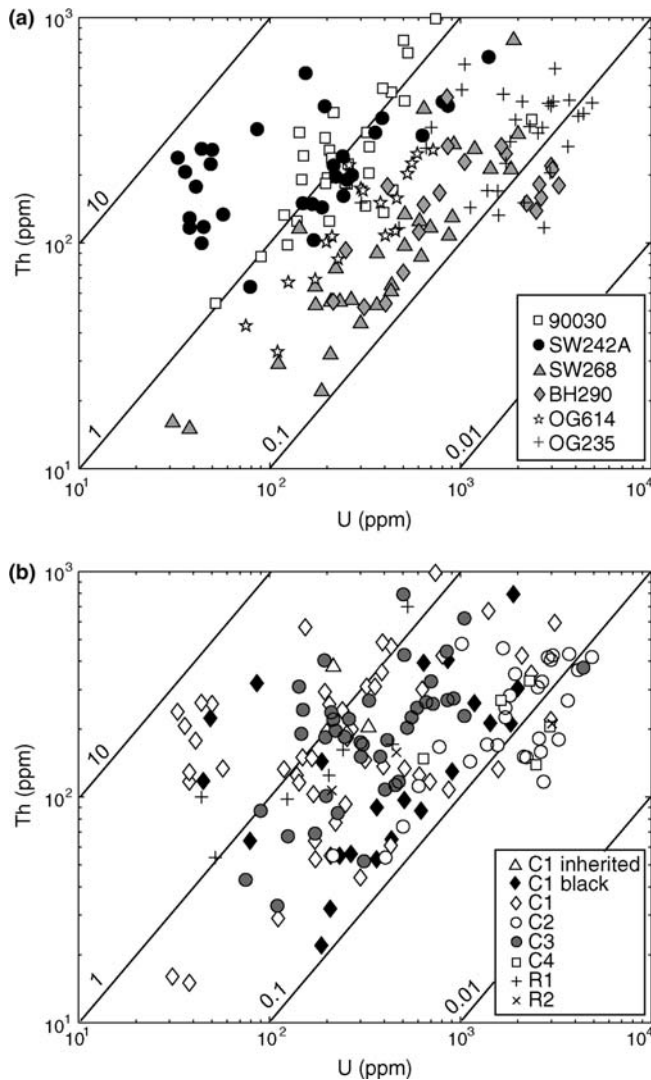


**Fig. 4** **a** Th–U plot for all analyses grouped by sample. **b** Th–U plot for all analyses grouped by zircon type as defined in the text

The rock crystallised at or before ca. 3,550 Ma. However, sample OG615 from the same location gave a minimum age for the precursor to the orthogneiss at ca. 3,655 Ma (Kelly 2000). Internal zoning of these C3 cores indicates that they crystallised in the presence of melt, consistent with the development of an early leucocratic segregations in this lithology. A cluster of 5 C3 concordant analyses between ca. 3,480–3,400 Ma and a spread of data down to ca. 3,200 Ma may represent the effects of Pb-loss, after their growth at ca. 3,480 Ma. Kelly (2000) inferred partial to total resetting of older zircon ages at ca. 3,470 Ma on the basis of U–Pb SHRIMP data from sample OG615. The two R2 metamorphic rims that trend towards ca. 1,200 Ma may indicate a younger metamorphic event at this time, but there is no evidence for the growth or modification of zircon at this time in other samples from the Oygarden Group. It seems likely that these rims have ‘mixed’  $^{207}\text{Pb}/^{206}\text{Pb}$  ages, artefacts of several Pb-loss events.

#### *BH290 - pre- $D_2$ homogenous felsic orthogneiss, Havstein Island*

Twenty-one analyses of 21 zircons were obtained for sample BH290 (ETable 3; Electronic Supplementary Material). Like the two previous samples, results from BH290 show a series of discordant analyses that represent a protracted history of tectonothermal events (Fig. 5c). The oldest analysis has a  $^{207}\text{Pb}/^{206}\text{Pb}$  age of  $3,538 \pm 7$  Ma (number 22; C3) and is nearly concordant. The young group of data (inset Fig. 5c) consist of metamorphic C2 and C4 cores. The youngest analysis (number 23; C2) has a near-concordant age of  $944 \pm 11$  Ma.

Complex U–Pb zircon data from sample BH290 indicate it is composed, at least in part, of reworked Archaean rocks with a minimum  $^{207}\text{Pb}/^{206}\text{Pb}$  age of ca. 3,540 Ma. These zircon grains experienced multiple stages of disturbance in the Archaean and Proterozoic. Several concordant analyses (numbers 3, 5 and 17; C2) between ca. 2,950–2,740 Ma may reflect the effects of metamorphism at this time; like sample OG235 it is not possible to attribute these zircon ages to a single event. The trend of analyses to ca. 940 Ma is interpreted to be associated with the deformation and metamorphism during the RSE and is identical to a U–Pb zircon age of  $940 \pm 80$  Ma from a syn-tectonic pegmatite in the Stillwell Hills (Grew et al. 1988).

#### *SW268 – pre- $D_2$ Stillwell Hills Orthogneiss, Stillwell Hills*

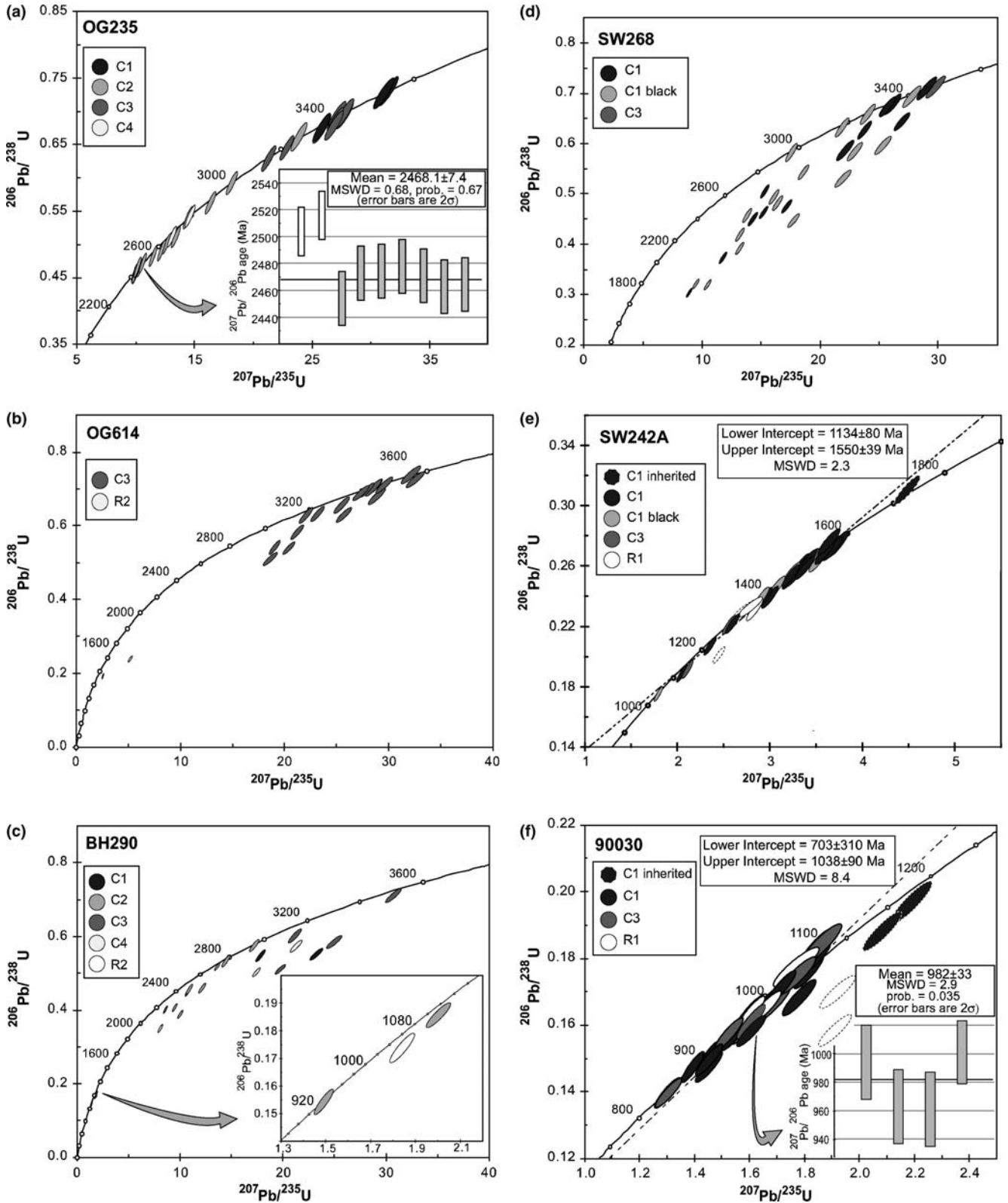
Thirty-one analyses of 24 zircons were obtained for SW268 (ETable 4; Electronic Supplementary Material). Though most analyses are profoundly discordant, they trend along a scattered discordia from ca. 3,460 Ma (Fig. 5d). The oldest analysis (number 28; C3) has an age of  $3,457 \pm 9$  Ma. The analyses broadly project towards a Neoproterozoic lower intercept (Fig. 5d).

U–Pb zircon analyses for SW268 indicate that protoliths to the dominant layered orthogneiss in the Stillwell Hills were older than ca. 3,460 Ma. A spread of near-concordant data down to  $2,971 \pm 9$  Ma (number 13; C1 black) could be consistent with isotopic resetting at ca. 2,970 Ma. However, as there is not a tight clustering of data there is no definitive evidence for an event at this time. The trend in  $^{207}\text{Pb}/^{206}\text{Pb}$  ages is inferred to reflect isotopic disturbance during the RSE.

#### *SW242A - pre- $D_3$ K-feldspar megacrystic charnockite, Stillwell Hills*

Thirty-one analyses were obtained from 26 zircons in SW242A (ETable 5; Electronic Supplementary Material) and results lie on or very close to concordia (Fig. 5e). The chord, with intercepts of  $1,550 \pm 39$  and  $1,134 \pm 80$  Ma, has been calculated using analyses from C1 and C1 black cores, excluding a xenocrystic zircon





(number 30) and two discordant analyses (numbers 10 and 12).

It is probable that emplacement of the charnockite occurred before ca. 1,550 Ma in the Stillwell Hills. These

results contrast a spread of ca. 960–915 Ma concordant ages for type C3 and C4 zircons presented for the same unit by Kelly et al. (2002; U–Pb SHRIMP data). This sample showed no evidence of Mesoproterozoic aged

**Fig. 5 a** Standard Wetherill concordia diagram showing the distribution of U–Pb zircon analyses for sample OG235. The broad spread of data lies on or close to concordia. Inset shows a weighted average for seven analyses at ca. 2,740 Ma. Numbers 5 and 11 were omitted as their inclusion gives a result outside two  $2\sigma$  of the mean (shown in white). **b** Standard Wetherill concordia diagram showing the distribution of U–Pb zircon analyses for sample OG614. The data are spread close to concordia between ca. 3,550–3,150 Ma and give a Pb-loss trend towards ca. 1,200 Ma. **c** Standard Wetherill concordia diagram showing the distribution of U–Pb zircon analyses for sample BH290. Most of the data are profoundly discordant reflecting several periods of Pb-loss and isotopic resetting from ca. 3,540 Ma. Inset shows detail at the lower intercept of a regression line to ca. 940 Ma. **d** Standard Wetherill concordia diagram showing the distribution of U–Pb zircon analyses for sample SW268. Though the data are significantly discordant, most analyses trend from ca. 3,460 Ma towards a Neoproterozoic lower intercept. A spread of concordant and near-concordant data can be seen from ca. 3,460 to ca. 2,970 Ma. **e** Standard Wetherill concordia diagram showing the distribution of U–Pb zircon analyses for sample SW242A. C1 analyses only were used in intercept calculations, excluding xenocrystic and extremely discordant data (see text for discussion). **f** Standard Wetherill concordia diagram showing the distribution of U–Pb zircon analyses for sample 90030. C1 analyses only were used in intercept calculations, excluding xenocrystic and extremely discordant data (see text for discussion). *Inset* shows a weighted average for the main population of four analyses

zircon grains. Kelly et al. (2002) suggested that this may be due to the recrystallisation of xenocrystic zircon from the lower crustal source of the charnockite, or earlier magmatic xenocrysts, being partially reset during the intrusion of the charnockite. In this case the ca. 915 Ma age would represent a minimum crystallisation age of the charnockite. The results are also consistent with the partial resetting of post-intrusion (ca. 960 Ma) magmatic zircon during metamorphism at ca. 915 Ma. Though the sample used in the two studies are from the same unit, their zircon morphology is markedly different. SW242 (Kelly et al. 2002) does not preserve magmatic type zircons whereas zircons analysed in this study are dominated by such grains. The abundance of C1 cores together with a low D3-strain setting for the location of sample SW242A suggests that emplacement of the charnockite occurred before ca. 1,550 Ma (concordia upper intercept). If this is the case, it is tempting to suggest that ca. 1,600 Ma metamorphism in the nearby Oygarden Islands (Kelly et al. 2002) may be associated with the intrusion of this charnockite body, or vice versa.

#### 90030 - pre-D<sub>3</sub> Mawson Charnockite, Mawson Station

Thirty-one analyses were made of 26 zircons for sample 90030 (ETable 6; Electronic Supplementary Material). Calculations were based on C1 analyses only, excluding two xenocrystic zircons and analysis number 35 due to discordance (Fig. 5f). The upper and lower intercepts are  $1,038 \pm 90$  and  $703 \pm 310$  Ma respectively.

Our U–Pb results agrees well with previous interpretations for the age of the Mawson Charnockite (Black et al. 1987; Young and Black 1991). An error-weighted mean of the main C1 population (inset Fig. 5f)

gives a crystallisation age for 4 C1 core analyses at  $982 \pm 33$  Ma. However, the spread of much of the data close to concordia may be due to isotopic disturbance during the RSE soon after emplacement, or may represent a mix of inherited zircon data, isotopic resetting and new zircon growth. Emplacement of the charnockite is interpreted to have accompanied or immediately followed peak metamorphic conditions (syn/post D<sub>2</sub>, pre-D<sub>3</sub>; Clarke 1988). Felsic magmatism at this time is also recorded at Cape Bruce during the onset of the RSE (Dunkley 1998; Dunkley et al. 2003).

#### Hf isotope data

In-situ hafnium analyses for terrane characterisation is a relatively new technique made available with advances in LAM-MC-ICPMS. Zircon grains, which have low Lu/Hf, record the initial Hf isotope composition of the magmatic system, and are resistant to ‘resetting’ by later metamorphic events. However new growth of zircon after magmatic crystallisation (rims or new grains) may contain different amounts of radiogenic Hf reflecting the contribution of phases with higher Lu/Hf than the zircon (Kinny et al. 1991; Hoskin and Black 2000; Zheng et al. 2004).  $^{176}\text{Lu}$  decays to  $^{176}\text{Hf}$  and the fractionation of these elements during partial melting leaves melts with a low Lu/Hf ratio and residue with high Lu/Hf ratios. Variations in  $^{176}\text{Hf}/^{177}\text{Hf}$  ratios are sensitive to the relative involvement of old crust (low  $^{176}\text{Hf}/^{177}\text{Hf}$ ) versus juvenile crust derived from a depleted mantle (high  $^{176}\text{Hf}/^{177}\text{Hf}$ ). Lu–Hf isotopic data are presented in ETable 7 (Electronic Supplementary Material) and in Fig. 6. The dotted lines in Fig. 6 show the evolution for a rock with  $^{176}\text{Lu}/^{177}\text{Hf}=0.015$  (samples OG235, OG614, BH290, SW268) corresponding to the average crust and  $^{176}\text{Lu}/^{177}\text{Hf}=0.010$  for more felsic rocks (OG235, SW242A, 90030) (Griffin et al. 2002; Zheng et al. 2004).

The  $^{176}\text{Hf}/^{177}\text{Hf}$ – $^{207}\text{Pb}/^{206}\text{Pb}$  age distributions for orthogneiss samples OG235 and SW268 are essentially flat (i.e. zircons have very similar  $^{176}\text{Hf}/^{177}\text{Hf}$  ratios irrespective of their age); zircon ages in these ranges are probably recrystallised rather than representing new growth events. Hf analyses for sample OG235 include metamorphic C2 and C4 zircons that are concordant or nearly concordant (ETable 7; Electronic Supplementary Material). Analyses in the youngest cluster of data (ca. 2,450–2,550 Ma) are part of a concordant cluster (Fig. 5a). These zircons are interpreted to have recrystallised during ca. 2,470 Ma metamorphism as the span of Hf ratios of these zircons ( $^{176}\text{Hf}/^{177}\text{Hf}=0.280433$ – $0.280547$ ) include the Hf ratio of the oldest zircon analysed ( $^{176}\text{Hf}/^{177}\text{Hf}=0.280527$ ). Hf isotope analyses from C1 and black C1 zircon cores in sample SW268 (ETable 7; Electronic Supplementary Material) can be modelled with a protolith age very similar to that of OG235. Two lines have been fitted to the data as the samples are relatively felsic and may be better repre-



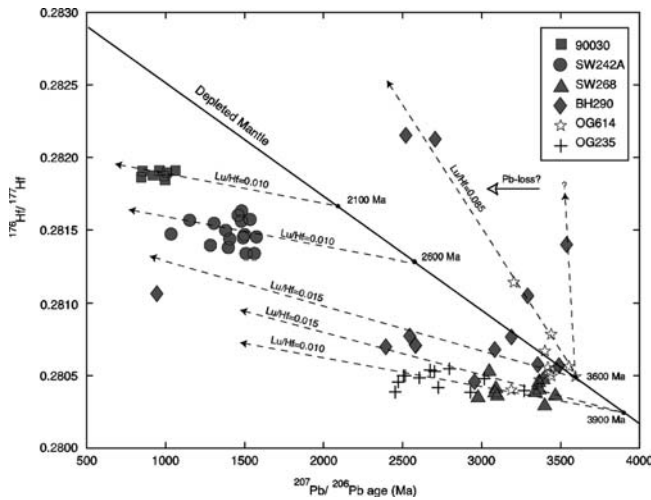


**Fig. 6**  $^{176}\text{Hf}/^{177}\text{Hf}$  vs.  $^{207}\text{Pb}/^{206}\text{Pb}$  ages for all samples with the depleted mantle reference line ( $\text{Lu}/\text{Hf}=0.0384$ ). Zircon analyses with similar Hf isotopic compositions but different ages lie along the indicated evolution lines. Zircons with high radiogenic Hf probably grew during the breakdown of garnet

sented by  $^{176}\text{Lu}/^{177}\text{Hf}=0.010$ . The Hf isotopic ratios for the oldest zircons in both these samples lie well below the depleted mantle curve, indicating they were derived by the remelting of older material. The minimum protolith age ( $T^{\text{Hf}}_{\text{DM}}$ ) assuming derivation from a depleted mantle source is ca. 3,700 Ma or closer to ca. 3,900 Ma if the protolith had the  $\text{Lu}/\text{Hf}=0.015\text{--}0.010$ .

Hf isotope analyses for sample OG614 are exclusively from zircon grains with concordant or near-concordant C3 ages (ETable 7; Electronic Supplementary Material). Sample BH290 has similar  $^{176}\text{Hf}/^{177}\text{Hf}$  ratios, but the Hf isotope analyses are associated with discordant  $^{207}\text{Pb}/^{206}\text{Pb}$  ages from C1, C2, C3 and C4 cores (ETable 7; Electronic Supplementary Material). A regression for analyses below the depleted mantle reference line is centred on the main cluster of concordant to near-concordant data at ca. 3,450 Ma. A crustal average  $T^{\text{Hf}}_{\text{DM}}$  age of ca. 3,600 Ma is obtained for a protolith with  $^{176}\text{Lu}/^{177}\text{Hf}=0.015$  (Fig. 6). The oldest zircons in samples OG614 and BH290 contain a higher proportion of radiogenic Hf than samples OG235 and SW268 and therefore may represent primary mantle melts at ca. 3,600 Ma. The zircon resetting/recrystallisation over ca. 300 Myr suggests that all these rocks were in the deep crust.

The charnockitic samples 90030 and SW242A have much higher  $^{176}\text{Hf}/^{177}\text{Hf}$  ratios than the older rocks. Hf isotope analyses from zircon in sample SW242A were taken from magmatic C1 and C3 zircons with concordant or near-concordant ages (ETable 7; Electronic Supplementary Material). We have modelled these data with  $^{176}\text{Lu}/^{177}\text{Hf}=0.010$ ; this gives a protolith  $T^{\text{Hf}}_{\text{DM}} \approx 2,600$  Ma (Fig. 6). SW242A may have been derived from a source with an age and Hf isotope composition like orthogneiss samples OG614 and BH290, but only if this source was more mafic ( $^{176}\text{Lu}/^{177}\text{Hf}=0.02$ ) than

**Fig. 7** Time-space diagram summarizing the geochronological data for Kemp and MacRobertson Land. Protolith ranges incorporate  $T^{\text{Hf}}_{\text{DM}}$  ages as well as  $T^{\text{Hf}}_{\text{DM}}$  crustal average estimates (maximum age). Where  $T^{\text{Hf}}_{\text{DM}}$  age ranges are large, U–Pb minimum emplacement age is taken as a source minimum age (OG614, BH290). Lithologies are felsic orthogneisses unless otherwise stated. Reference numbers refer to the same references as cited for Table 1

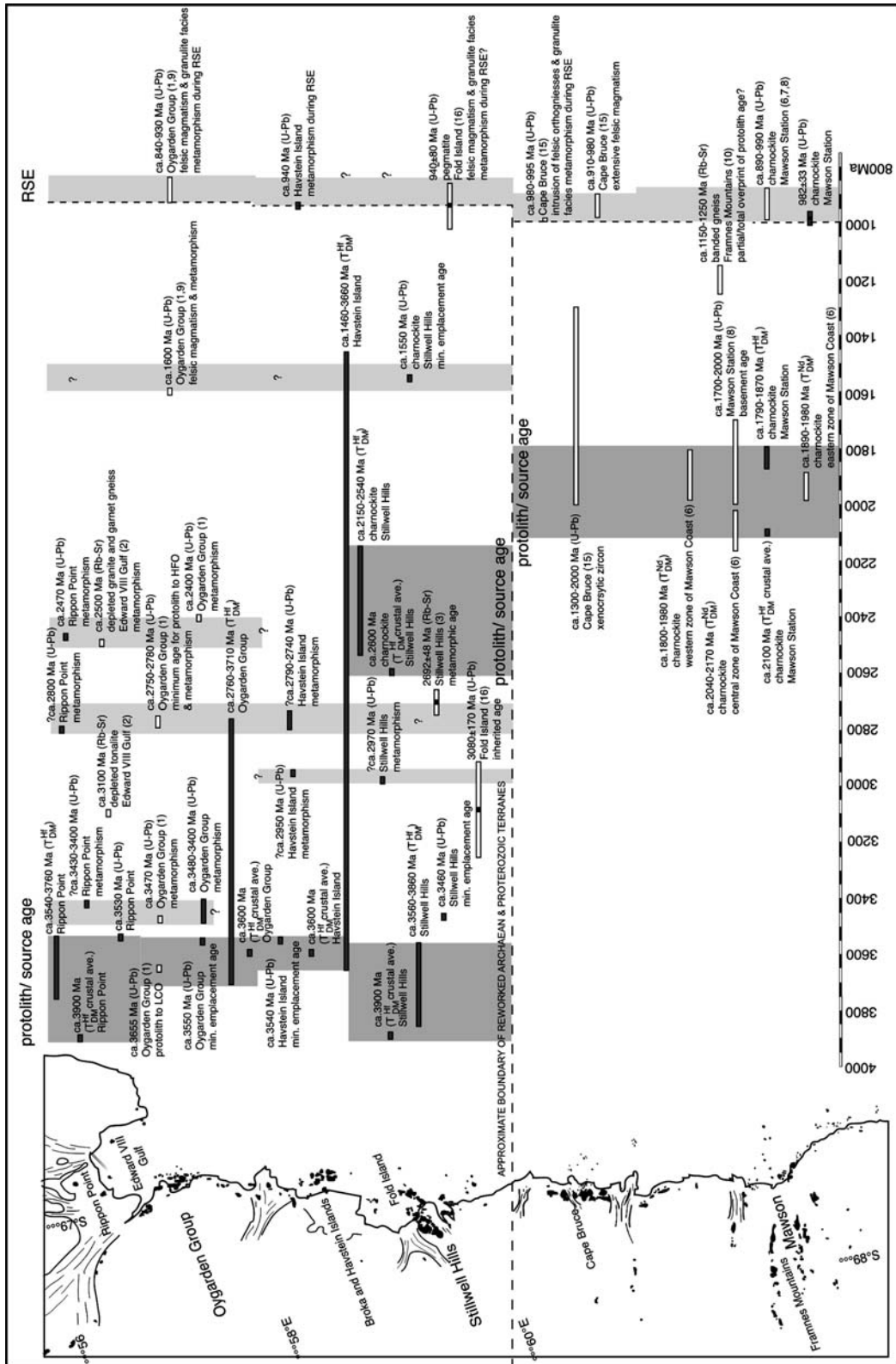
those samples. Alternatively, SW242A could be derived from a mixture of juvenile magmas and material from a more felsic, older lower crust. Similarly, charnockitic sample 90030 has very near-concordant magmatic C1 and C3 core zircon data (ETable 7; Electronic Supplementary Material) that can be modelled with a protolith  $^{176}\text{Lu}/^{177}\text{Hf}=0.010$ , to give a  $T^{\text{Hf}}_{\text{DM}} \approx 2,100$  Ma (Fig. 6). The high  $^{176}\text{Hf}/^{177}\text{Hf}$  ratios of zircons from sample 90030 require either a younger source, or a mixing between juvenile and ancient components.

Several analyses contain unusual zircons with highly radiogenic Hf (OG614 and BH290), lying well above the DM curve. A regression through these points gives,  $T^{\text{Hf}}_{\text{DM}} \approx 3,600$  Ma and a  $^{176}\text{Lu}/^{177}\text{Hf}$  ratio of 0.085. Such a high  $\text{Lu}/\text{Hf}$  ratio is likely to be attributed to a phase such as garnet (e.g. Duchene et al. 1997). OG614 contains trails of garnet and orthopyroxene that define a penetrative S1 foliation, whereas BH290 contains trails of garnet defining an S2 foliation. It is likely that the breakdown of down of some of this garnet, with a high  $^{176}\text{Lu}/^{177}\text{Hf}$  ratio, during granulite facies metamorphism has liberated Lu and resulted in the growth of zircons enriched in  $^{176}\text{Hf}$ . These samples are therefore interpreted as containing zircon that formed before ca. 3,550 Ma (OG614) and ca. 3,540 Ma (BH290) both by recrystallisation of older (ca. 3,600 Ma) zircon, and by growth from Zr (and Hf) liberated through the breakdown of garnet. It is also possible that the high  $^{176}\text{Hf}/^{177}\text{Hf}$  analyses of two metamorphic zircons from sample BH290 (numbers 28 and 8; ETable 7; Electronic Supplementary Material) may be from recrystallised zircons from a still higher  $^{176}\text{Lu}/^{177}\text{Hf}$  trend, shown on the right of Fig. 6.

## Discussion

A chronology of events for the Rayner Complex and implications for crustal evolution

Figure 7 is a time-space diagram that outlines the main isotopic data for rocks from the MacRobertson and Kemp Land Coast. Zircon ages and Hf source ages for the felsic orthogneisses are at least partially coeval at ca. 3,660–3,560 Ma, and possibly extend as far back as ca. 3,900 Ma in the western part of the study area. They indicate a similar crustal source for rocks felsic orthogneisses from Rippon Point, the Oygarden Group, Broka and Havstein Islands and the Stillwell Hills (Fig. 7). The oldest ages obtained from rocks of the Napier Complex



come from ca. 3,850–3,770 Ma precursors to felsic gneiss in the Tula Mountains (Harley and Black 1997; Kelly and Harley 2004); crustal growth initiated before this. An emplacement age of ca. 3,530 Ma for an orthogneiss at Rippon Point in the Napier Complex does not

correlate with emplacement ages of these more ancient crustal fragments, nor numerous late Archaean (ca. 3,100–2,450 Ma) areas of the Napier Complex (e.g. Sheraton et al. 1987; Harley and Black 1997; Hokada et al. 2003). This age is close to emplacement ages for

felsic orthogneisses from the neighbouring Rayner Complex (e.g. Kelly 2000; Kelly et al. 2002; this study). Zircons from felsic orthogneisses in the Oygarden Group give a minimum emplacement age of ca. 3,550 Ma (this study) and probably at least ca. 3,655 Ma (Kelly 2000). CHIME ages from zircon cores from metapelite at Mt. Cronus in the Napier Complex give an age of  $3,646 \pm 136$  Ma, a minimum age for the protolith or source region (Asami et al. 1998). A thermal event ca. 3,480–3,400 Ma is interpreted to correlate with a ca. 3,470 Ma isotopic disturbance in OG615, possibly reflecting the development of an  $S_1$  foliation and alignment of early leucosomes (N.M. Kelly, personal communication).

A reinterpretation of isotopic data presented by Harley and Black (1997) by Kelly and Harley (2004) highlights a ca. 2,990 Ma magmatic episode in some parts of the Napier Complex (Proclamation Island and Dallwitz Nunatak; Kelly and Harley 2004). Though some Kemp Land analyses give concordant or near concordant ages close to this (OG235, BH290 and SW268), no conclusive evidence of this event was found in this study. Near-concordant ages from the Rippon Point orthogneiss between ca. 3,530–2,470 Ma could correlate with the ca. 2,750–2,780 Ma thermal disturbance recorded in the nearby Oygarden Group (Kelly 2000). A similar distribution in data from Havstein Island may also indicate some sort of thermal event at this time and possibly even relate to the whole rock Rb–Sr age of  $2,692 \pm 48$  Ma recorded in the Stillwell Hills (Clarke 1987). Effects of ca. 2,500–2,450 Ma metamorphism in the Napier Complex (e.g. Grew and Manton 1979; Grew 1998; Carson et al. 2002; Hokada et al. 2003, 2004) are evident in ca. 2,470 Ma zircon ages at Rippon Point (this study) and other rocks in Edward VIII Gulf (Sheraton and Black 1983) and the Oygarden Group (Kelly 2000; Kelly et al. in press). Whether this age dates UHT metamorphism in the Napier Complex, or post-UHT zircon growth is still a matter of debate (see recent papers by Harley et al. 2001, Hokada et al. 2003, 2004; Kelly and Harley 2004).

The charnockite bodies at Mawson Station and in the Stillwell Hills have Hf ratios and source ages that are markedly different, both from each other, and the older orthogneisses discussed above. Charnockite in the Stillwell Hills intrudes the early Archaean Stillwell Hills Orthogneiss but does not show isotopic or xenolithic evidence for a source age older than ca. 2,600 Ma (Fig. 7). This is in contrast to model ages for the Mawson Charnockite that correlate well with radiometric ages for the host rock (Fig. 7). This could indicate derivation via partial melting of a more mafic lower crustal source of similar age, perhaps without the addition of more primitive mantle components, as proposed for charnockitic bodies in the nPCM (Young et al. 1997; Zhao et al. 1997).

Mechanisms for such crustal growth in the Rayner Complex have been likened to those presented for other Proterozoic belts around the world, involving a mosaic of crustal domains with distinct sources and evolutionary histories (Young et al. 1997; Zhao et al. 1997). The tec-

tonic setting for such a complexly accreted terrane remains unclear. Calc-alkaline geochemical signatures of charnockite at Mawson Base and in the nPCM are consistent with Proterozoic crustal growth along an active compressional plate margin (Young and Ellis 1991; Zhao et al. 1997). Island arc and volcanic-arc magmatism may be responsible for metavolcanics and granitic intrusives at Fisher Massif in the nPCM (Mikhalsky et al. 1996, 2001). As discussed by Kelly et al. (2002), ca. 1,600 Ma ages that represent a minor thermal event in the Oygarden area are also found in the Eastern Ghats Province and provide significant regional tectonic correlation before final amalgamation during the RSE. They suggest that this part of western Kemp Land, and most probably the Napier Complex, were part of an Eastern Ghats terrain at or before ca. 1,600 Ma and may represent the initial stages of an extended amalgamation that continued through into the Neoproterozoic. The intrusion of a charnockitic body before ca. 1,550 Ma in the Stillwell Hills is tentatively correlated with this ca. 1,600 Ma event in the Oygarden Group. However, no indication of a thermal event at this time can be present in data from Archaean orthogneisses from the Stillwell Hills or Havstein Island, despite the very similar model source ages. This may be due to disturbance during the RSE, though any confident interpretation of effects of the RSE is limited by the complex Pb-loss record. Whereas orthogneiss from the Oygarden Group and the Stillwell Hills records isotopic disturbances that trend to Neoproterozoic ages, the sample from the Broka-Havstein Islands was the only lithology to preserve a ca. 940 Ma concordant analysis. The intrusion of the Mawson Charnockite at  $982 \pm 33$  Ma and a probable thermal disturbance experienced by these zircons soon after crystallisation supports the initiation of the RSE in the Mawson and Cape Bruce area some 40–50 Myr earlier than the onset of the RSE in Kemp Land (Fig. 7; Kelly et al. 2002).

Isotopic data presented in this study indicate that Kemp Land evolved as a separate terrane from the rest of the Rayner Complex. The data suggest that this region represents a part of the Napier Complex rocks that was tectonically reworked in the Neoproterozoic, specifically during the ca. 940–900 Ma RSE. Rocks to the east of the Stillwell Hills represent Mesoproterozoic crust accreted to a complexly deformed Archaean craton after ca. 1,600 Ma, as there is no record of a metamorphic event at this time in MacRobertson Land. The absence of outcrop between the Stillwell Hills and Cape Bruce (Fig. 7) does not allow an accurate demarcation of the accretionary margin. Model ages of source rocks for exposures elsewhere in the Rayner Complex (western Enderby Land and the nPCM) also indicate extensive Meso-Palaeoproterozoic crustal growth (Black et al. 1987; Zhao et al. 1997).

**Acknowledgements** Careful reviews by S. Harley and an anonymous reviewer improved the paper. This work was completed with funding from the Antarctic Science Advisory Committee (GLC: ASAC Project No. 1150). Samples were collected during the 1996/

1997, 1997/1998, 1999/2000 Australian National Antarctic Research Expeditions. The authors would like to thank the Australian Antarctic Division and the personal of Mawson Base for their logistic support. JAH and CLK were supported by Australian Postgraduate Awards at the University of Sydney. Norm Pearson provided considerable assistance and guidance in the analytical work and its interpretation. Nigel Kelly, Julie Hollis, Richard White, Vanessa Bennett and Joel Fitzherbert are thanked for their assistance in the collection of samples. This is contribution No. 372 from the ARC National Key Centre for Geochemical Evolution and Metallogeny of Continents (<http://www.els.mq.edu.au/GE-MOC/>).

## References

- Anderson T (2002) Correction of common lead in U–Pb analyses that do not report  $^{204}\text{Pb}$ . *Chemical Geology* 192:59–79
- Arriens PA (1975) Precambrian geochronology of Antarctica (abstract). In: 1st Australian Geological Convention, Geological Society of Australia, Adelaide, pp 97–98
- Asami M, Suzuki S, Grew ES, Adachi M (1998) CHIME ages for granulites from the Napier Complex, east Antarctica. *Polar Geoscience* 11:172–199
- Belousova EA, Griffin WL, Shee SR, Jackson SE, O'Reilly SY (2001) Two age populations of zircons from the Timber Creek kimberlites, Northern Territory, as determined by laser-ablation ICP-MS analysis. *Australian J Sciences* 48:757–765
- Bizzarro EA, Baker JA, H H, Ulfbeck D, Rosing M (2003) Early history of the Earth's crust-mantle system inferred from hafnium isotopes in chondrites. *Nature* 421:931–933
- Black LP, Gulson BL (1978) The age of the Mud Tank carbonatite, Strangways Range, Northern Territory. Bureau of Mineral Resources, *Journal of Australian Geology and Geophysics* 3:227–232
- Black LP, Williams IS, Compston W (1986) Four zircon ages from one rock: the history of a 3930 Ma-old granulite from Mount Sones, Enderby Land, Antarctica. *Contributions to Mineralogy and Petrology* 94:427–437
- Black LP, Harley SL, Sun SS, McCulloch MT (1987) The Rayner Complex of East Antarctica: complex isotopic systematics within a Proterozoic mobile belt. *Journal of Metamorphic Geology* 5:1–26
- Blichert-Toft J, Chauvel C, Albarède F (1997) The Lu–Hf geochemistry of chondrites and the evolution of the mantle-crust system. *Earth and Planetary Science Letters* 148:243–258. Erratum
- Boger SD, Carson CJ, Wilson CJL, Fanning CM (2000) Neoproterozoic deformation in the Radok Lake region of the northern Prince Charles Mountains, east Antarctica; evidence for a single protracted orogenic event. *Precambrian Research* 104(1–2):1–24
- Carson CJ, Boger SD, Fanning CM, Wilson CJL, Thost DE (2000) SHRIMP U–Pb geochronology from Mount Kirkby, northern Prince Charles Mountains, East Antarctica. *Antarctic Science* 12(4):429–442
- Carson CJ, Ague JJ, Coath CD (2002) U–Pb geochronology from Tonagh Island, East Antarctica: implications for the timing of ultra-high temperature metamorphism of the Napier Complex. *Precambrian Research* 116:237–263
- Clarke GL (1987) A comparative study of the structural and metamorphic evolution of the Olary (South Australian) and Stillwell Hills (Antarctica) Precambrian terrains. Ph.D. thesis, The University of Melbourne, Melbourne, 254 pp
- Clarke GL (1988) Structural constraints on the Proterozoic reworking of Archaean crust in the Rayner Complex, MacRobertson and Kemp Land coast, East Antarctica. *Precambrian Research* 40–41:137–156
- De Bièvre P, Taylor PDP (1993) Table of the isotopic composition of the elements. *International Journal of Mass Spectrometry and Ion Processes* 123(2):149–166
- Duchene S, Blichert-Toft J, Luais B, Telouk P, Lardeaux JM, Albarède F (1997) The Lu–Hf dating of garnets and the ages of the Alpine high-pressure metamorphism. *Nature* 387:586–589
- Dunkley DJ (1998) The Rayner Complex in MacRobertson Land, east Antarctica. Ph.D. thesis, The University of Sydney, Sydney, 284 pp
- Dunkley DJ, Clarke GL, White RW (2002) Structural and metamorphic evolution of the mid-late Proterozoic Rayner Complex, East Antarctica. In: Gamble JA, Skinner DNB, Henrys S (eds) *Antarctica at the Close of a Millennium. Proceedings Volume 8th International Symposium on Antarctic Earth Sciences*, Royal Society of New Zealand Bulletin. The Royal Society of New Zealand, pp 31–42
- Dunkley DJ, Clarke GL, White RW (2003) The ~1020–900 Ma Rayner Structural Episode in MacRobertson Land, east Antarctica: a case of oblique continental collision? *Proceedings of the 8th International Symposium on Antarctic Earth Sciences*, Wellington, New Zealand, 1999, The Royal Society of New Zealand Bulletin 35:31–42
- Fitzsimons ICW (2000) A review of tectonic events in the East Antarctic Shield and their implications for Gondwana and earlier supercontinents. *J Afr Earth Sci* 31(1):3–23
- Grew ES (1998) Boron and beryllium minerals in granulite-facies pegmatites and implications of beryllium pegmatites for the origin and evolution of the Archaean Napier Complex of East Antarctica. *Memoirs of the National Institute of Polar Research, Special Issue* 53:74–92
- Grew ES, Manton WI (1979) Archaean rocks in Antarctica: 2.5 billion-year uranium-lead ages of pegmatites in Enderby Land. *Science* 206:443–445
- Grew ES, Manton WI, James PR (1988) U–Pb data on granulite facies rocks from Fold Island, Kemp Coast, east Antarctica. *Precambrian Research* 42:63–75
- Griffin WL, Pearson NJ, Belousova EA, Jackson SE, van Acherbergh E, O'Reilly SY, Shee SR (2000) The Hf isotope composition of cratonic mantle: LAM-MC-ICPMS analysis of zircon megacrysts in kimberlites. *Geochimica et Cosmochimica Acta* 64(1):133–147
- Griffin WL, Wang X, Jackson SE, Pearson NJ, O'Reilly SY, Xu X, Zhou X (2002) Zircon chemistry and magma mixing, SE China: In-situ analysis of Hf isotopes, Tonglu and Pingtan igneous complexes. *Lithos* 61:237–269
- Harley SL, Black LP (1997) A revised Archaean chronology for the Napier Complex, Enderby Land, from SHRIMP ion-microprobe studies. *Antarc Sci* 9(1):74–91
- Harley SL, Kinny PD, Snape I, Black LP (2001) Zircon chemistry and the definition of events in Archaean granulite terrains. In: Cassidy KF, Dunphy JM, van Kranendonk MJ (eds) *4th International Archaean Symposium, Extended Abstract Volume*, AGSO Geoscience Australia record 2001/37, Canberra, pp 511–513
- Hirata T, Nesbitt RW (1995) U–Pb isotope geochronology of zircon: Evaluation of the laser probe-inductively coupled plasma-mass spectrometry technique. *Geochim Cosmochim Acta* 59:2491–2500
- Hokada T, Misawa K, Shiraishi K, Suzuki S (2003) Mid to late Archaean (3.3–2.5 Ga) tonalitic crustal formation and high-grade metamorphism at Mt. Riiser-Larsen, Napier Complex, East Antarctica. *Precamb Res* 127:215–228
- Hokada T, Misawa K, Yokoyama K, Shiraishi K, Yamaguchi A (2004) SHRIMP and electron microprobe chronology of UHT metamorphism in the Napier Complex, East Antarctica: implications for zircon growth at >1,000°C. *Contrib Mineral Petrol* 147:1–20
- Hoskin PWO, Black LP (2000) Metamorphic zircon formation by solid-state recrystallization of protolith igneous zircon. *J Metamorphic Geol* 18:423–439
- Jackson SE, Dunning GR, Horn I, Ingo, Longereich HP (1997) The application of laser ablation microprobe (LAM)-ICP-MS to in situ U–Pb zircon geochronology: Keynote address. In: GAC/MAC joint annual meeting, May 1997, Ottawa, Ontario, p A73



- Jackson SE, Pearson NJ, Griffin WL, Belousova EA (2004) The application of Laser Ablation-Inductively Coupled Plasma-Mass Spectrometry (LA-ICP-MS) to in situ U–Pb zircon geochemistry. *Chem Geol* (in press)
- Kamenev EN (1972) Geological structure of Enderby Land. In: Antarctic geology and geophysics. International Union of Geological Sciences (IUGS), Oslo, International, pp 579–583
- Kelly NM (2000) Deformation and metamorphism in the lower continental crust: Oygarden Group of Islands, east Antarctica. PhD Thesis, The University of Sydney, p 316
- Kelly NM, Harley SL (2004) An integrated textural and chemical approach to zircon geochronology: refining the Archaean history of the Napier Complex, east Antarctica. *Contrib Mineral Petrol* (in press)
- Kelly NM, Clarke GL, Carson CJ, White RW (2000) Thrusting in the lower crust: evidence from the Oygarden Islands, Kemp Land, East Antarctica. *Geol Mag* 137(3):219–234
- Kelly NM, Clarke GL, Fanning CM (2002) A two-stage evolution of the Neoproterozoic Rayner Structural Episode; new U–Pb sensitive high resolution ion microprobe constraints from the Oygarden Group, Kemp Land, East Antarctica. *Precamb Res* 116(3–4):307–330
- Kinny PD, Compston W, Williams IS (1991) A reconnaissance ion-probe study of hafnium isotopes in zircons. *Geochim Cosmochim Acta* 55:849–859
- Kinny PD, Black LP, Sheraton JW (1997) Zircon U–Pb ages and geochemistry of igneous and metamorphic rocks from the northern Prince Charles Mountains, Antarctica. *AGSO J Aust Geol Geophys* 16:637–654
- Knudsen T-L, Griffin WL, Hartz EH, Andresen A, Jackson SE (2001) In-situ hafnium and lead isotope analyses of detrital zircons from the Devonian sedimentary basin of NE Greenland: a record of repeated crustal reworking. *Contrib Mineral Petrol* 141:83–94
- Ludwig KR (2001) User manual for Isoplot/Ex, version 2.49, a geochronological toolkit for Microsoft Excel. Berkley Geochronological Centre Special Publication 1a
- Manton WI, Grew ES, Hoffman PF, Sheraton JW (1992) Granitic rocks of the Jetty Peninsula, Amery Ice Shelf area, East Antarctica. In: Yoshida Y, Kaminuma K, Shiraishi K (eds) Recent progress in Antarctic Earth Science. Terra Scientific Publishing Company, Tokyo, pp 179–189
- Mezger K, Krogstad EJ (1997) Interpretation of discordant U–Pb zircon ages: an evaluation. *J Metamorphic Geol* 15:127–140
- Mikhalsky EV, Sheraton JW, Laiba AA, Beliatsky BV (1996) Geochemistry and origin of Mesoproterozoic metavolcanic rocks from Fisser Massif, Prince Charles Mountains, east Antarctica. *Antarc Sci* 8:85–104
- Mikhalsky EV, Sheraton JW, Laiba AA, Tingey RJ, Thost DE, Kamenev EN, Fedorov LV (2001) Geology of the Prince Charles Mountains, Antarctica. *AGSO - Geoscience Australia Bulletin* 247, Canberra, Australia
- Norman MD, Pearson NJ, Sharma A, Griffin WL (1996) Quantitative analysis of trace elements in geological materials by laser ablation ICPMS: instrumental operating conditions and calibration values of NIST glasses. *Geostands Newslett* 20:247–261
- Pidgeon RT, Nemchin AA, Hitchen GJ (1998) Internal structures of zircons from Archaean granites from the Darling Range batholith: implications for zircon stability and the interpretation of zircon U–Pb ages. *Contrib Mineral Petrol* 132:288–299
- Rickers K, Mezger K, Raith MM (2001) Evolution of the Continental Crust in the Proterozoic Eastern Ghats Belt, India and new constraints for Rodinia reconstruction: implications from Sm–Nd, Rb–Sr and Pb–Pb isotopes. *Precamb Res* 112:183–210
- Rubatto D, Gebauer D (2000) Use of cathodoluminescence for U–Pb zircon dating by ion microprobe: some examples from the Western Alps. In: Pagel M, Barbin V, Blanc P, Ohnenstetter D (eds) *Cathodoluminescence in geosciences* Springer, Berlin Heidelberg New York, pp 373–400
- Rubatto D, Gebauer D, Fanning M (1998) Jurassic formation and Eocene subduction of the Zermatt-Saas- Fee ophiolites: implications for the geodynamic evolution of the Central and Western Alps. *Contrib Mineral Petrol* 132(3):269–287
- Sandiford M, Wilson CJL (1984) The structural evolution of the Fyfe Hills-Khmara Bay Region, Enderby Land, East Antarctica. *Aust J Earth Sci* 31(4):403–426
- Schaltegger U, Fanning CM, Günther D, Maurin JC, Schulmann K, Gebauer D (1999) Growth, annealing and recrystallization of zircon and preservation of monazite in high-grade metamorphism: conventional and in-situ U–Pb isotope, cathodoluminescence and microchemical evidence. *Contrib Mineral Petrol* 134:186–201
- Scherer E, Munker C, Mezger K (2001) Calibration of the lutetium–hafnium clock. *Science* 293:683–687
- Sheraton JW, Black LP (1981) Geochemistry and geochronology of proterozoic Tholeiite Dykes of East Antarctica: evidence for Mantle Metasomatism. *Contrib Mineral Petrol* 78:305–317
- Sheraton JW, Black LP (1983) Geochemistry of Precambrian gneisses: relevance for the evolution of the East Antarctic Shield. *Lithos* 16:273–296
- Sheraton JW, Offe LA, Tingey RJ, Ellis DJ (1980) Enderby Land, Antarctica—an unusual Precambrian high-grade metamorphic terrain. *J Geol Soc Aust* 27:1–18
- Sheraton JW, Tingey RJ, Black LP, Offe LA, Ellis DJ (1987) Geology of an unusual Precambrian high-grade metamorphic terrane—Enderby Land and western Kemp Land, Antarctica. *Australian Bureau of Mineral Resources Bulletin* vol 223, p 51
- Spetsius ZV, Belousova EA, Griffin WL, O'Reilly SY, Pearson NJ (2002) Archean sulfide inclusions in Paleozoic zircon megacrysts from the Mir kimberlite, Yakutia: implications for the dating of diamonds. *Earth Planet Sci Lett* 199:111–126
- Tingey RJ (1982) The geologic evolution of the Prince Charles Mountains—an Antarctic Archaean cratonic block. University of Wisconsin Press, Madison, pp 455–464
- Trail DS (1970) ANARE 1961 Geological Traverses on the Mac.Robertson Land and Kemp Land Coast. Bureau of Mineral Resources Geology and Geophysics Report vol 135, pp 1–32
- Vavra G, Gebauer D, Schmid R, Compston W (1996) Multiple zircon growth and recrystallization during polyphase Late Carboniferous to Triassic metamorphism in granulites of the Ivrea Zone (Southern Alps): An ion microprobe (SHRIMP) study. *Contrib Mineral Petrol* 122(4):337–358
- Vavra G, Schmid R, Gebauer D (1999) Internal morphology, habit and U–Th–Pb microanalysis of amphibolite-to-granulite facies zircons: geochronology of the Ivrea Zone (Southern Alps). *Contrib Mineral Petrol* 134(4):380–404
- Wiedenbeck M, Alle P, Corfu F, Griffin WL, Meier M, Oberli F, von Quadt A (1995) Three natural zircon standards for U–Th–Pb, Lu–Hf, trace element and REE analyses. *Geostands Newslett* 19:1–23
- Young DN, Black LP (1991) U–Pb zircon dating of Proterozoic igneous charnockites from the Mawson Coast, East Antarctica. *Antarc Sci* 3(2):205–216
- Young DN, Ellis DJ (1991) The intrusive Mawson charnockites: evidence for a compressional plate margin setting of the Proterozoic mobile belt of East Antarctica. In: Thomson MRA, Crame JA, Thomson JW (eds) *Geological evolution of Antarctica* Cambridge University Press, Cambridge, pp 25–31
- Young DN, Zhao J, Ellis DJ, McCulloch MT (1997) Geochemical and Sr–Nd isotopic mapping of source provinces for the Mawson charnockites, east Antarctica: implications for Proterozoic tectonics and Gondwana reconstruction. *Precamb Res* 86:1–19
- Zhao J, Ellis DJ, Kilpatrick JA, McCulloch MT (1997) Geochemical and Sr–Nd isotopic study of charnockites and related rocks in the northern Prince Charles Mountains, East Antarctica: implication for charnockite petrogenesis and Proterozoic crustal evolution. *Precamb Res* 81:37–66
- Zheng J, Griffin WL, O'Reilly SY, Lu F, Wang C, Zhang M, Wang F, Li H (2004) 3.6 Ga lower crust in central China: new evidence on the assembly of the North China craton. *Geology* 32(3):229–232